QCD field correlations in high-energy scattering

Erasmo Ferreira
Instituto de Física, Universidade Federal do Rio de Janeiro, Rio de Janeiro 21945-970, RJ, Brazil

Flávio Pereira
DAGE, Observatório Nacional, CNPq, Rio de Janeiro 20921-400, RJ, Brazil

(Received 8 July 1996)

The two independent correlation functions describing nonperturbative properties of the QCD vacuum are taken into account in the evaluation of the observables of soft high-energy hadron-hadron scattering. The model of the stochastic vacuum provides the framework in which a simple and effective description of the high-energy pp and $\overline{pp}$ data can be given, leading to a determination of relevant parameters of nonperturbative QCD and to a good description of the data. The ratio between the non-Abelian and the Abelian parts of the field correlations is studied in terms only of high-energy data and the results are compared to lattice calculations. It is shown that a slow increase of the hadronic radii with the energy accounts for the energy dependence of all observables. [S0556-2821(97)03101-9]

PACS number(s): 12.38.Lg, 13.85.Dz, 13.85.Lg

I. INTRODUCTION

Much effort has been made to describe the simple and universal features of high-energy hadronic scattering in terms of the fundamental theory of the strong interactions, and it is now understood that many important features are due to nonperturbative QCD effects. Among these attempts, we are here concerned with the application [1] of the model of the stochastic vacuum of nonperturbative QCD to hadron-hadron scattering. Soft processes, respecting (even microscopically) the quark and color confinement in the colliding hadrons, is a domain where the nonperturbative aspects of QCD can be explored and studied. This domain mixes the parameters describing properties of the QCD field (gluon condensate, correlation length) with those describing the colorless hadrons. The effective dynamics providing the basis for the phenomenological description of the data must have the characteristic features of the pomeron exchange mechanism of Regge phenomenology [2]: vacuum quantum numbers exchanged between well determined and unchanged hadronic structures. This mechanism leads, for all hadronic systems, to total cross-sections which increase with the energy [3] somewhat like $s^{0.0808}$. This behavior, which cannot be realistic for much higher energies, gives an adequate and simple description of the present data.

Several models relate the total high-energy cross sections to the hadronic radii [4]. This is a characteristic feature also of the model of the stochastic vacuum which gives specific predictions for the size dependence of the high-energy observables for different hadronic systems [1]. These predictions account for the observed ratios of πp to pp (or $\overline{pp}$) total cross sections, which have been thought of as indications supporting additive quark models, and also account for the important flavor dependence of the observables.

In the present work we deal with the pp and $\overline{pp}$ systems, describing the high-energy data in terms of nonperturbative QCD parameters, and relating the energy dependence of the observables with radius dependence. The knowledge of the hadronic structures required for the description of the soft high-energy data does not go beyond the information on their sizes, the simplest and most trivial transverse wave function giving all information required for the determination of the observables. We show that the energy dependence of the total cross section and of the forward slope parameter can both be accounted for by a slow variation of the radius associated with the transverse wave function.

The treatment of soft hadron-hadron scattering, essentially including the confinement properties of quantum chromodynamics, cannot be made straightforwardly, requiring use of approximations and models. The model of the stochastic vacuum, originally conceived to treat nonperturbative effects in low-energy hadron physics [5], was later applied to explain high-energy soft scattering [1]. The treatment is based on the concept of loop-loop scattering, which allows a gauge-independent formulation for the amplitudes. The loops, formed by the quark and antiquark lightlike paths in a moving hadron, have their contributions added incoherently, with their sizes weighed by transverse hadronic wave functions.

In the present work we present the results of a more complete calculation of the high-energy observables (total cross-section and slope parameter), in which both Abelian and non-Abelian contributions to the field correlator are taken into account. The role of the parameter κ measuring the strength of the non-Abelian part, which was determined in lattice calculations to be about 3/4, is studied and we observe that the range of values that suits the description of the high-energy data leads to a confirmation of the lattice results.

In the present analysis we take into account all available data on total cross sections and slope parameters in pp and $\overline{pp}$ scattering , which consist mainly [6,7] of CERN Intersecting Storage Rings (ISR) measurements at energies ranging from $\sqrt{s}=23$ GeV to $\sqrt{s}=63$ GeV, of the $\sqrt{s}=541-546$ GeV measurements in CERN Super Proton Synchrotron (SPS) and in Fermilab, and of the $\sqrt{s}=1800$ GeV information from the E-701 Fermilab experiment. These data are shown in Table I. In addition to these, there is

TABLE I. Experimental high-energy data from CERN ISR, CERN SPS, and Fermilab.

	$\sqrt{s}$ (GeV)	σ^T (mb)	B (GeV^{-2})	Ref. [6]
	23.5	39.65 ± 0.22	11.80 ± 0.30	(a)
	30.6	40.11 ± 0.17	12.20 ± 0.30	(a)
pp	45.0	41.79 ± 0.16	12.80 ± 0.20	(b)
	52.8	42.38 ± 0.15	12.87 ± 0.14	(a)
	62.3	43.55 ± 0.31	13.02 ± 0.27	(a)
	30.4	42.13 ± 0.57	12.70 ± 0.50	(a)
	52.6	43.32 ± 0.34	13.03 ± 0.52	(a)
$\overline{pp}$	62.3	44.12 ± 0.39	13.47 ± 0.52	(a)
	541	62.20 ± 1.50	15.52 ± 0.07	(c)
	546	61.90 ± 1.50	15.28 ± 0.58	(d)
	1800	72.20 ± 2.70	16.72 ± 0.44	(e)

a measurement [8] of $\sigma^T=65.3\pm2.3$ mb at $\sqrt{s}=900$ GeV and there are the measurements of $\sigma^T=80.6\pm2.3$ and $B=17.0\pm0.25$ GeV^{-2} at the Collider Detector at Fermilab (CDF) [9] at $\sqrt{s}=1800$ GeV which seem discrepant with the E-701 experiment at the same energy. A measurement by Burq *et al.* [10] at $\sqrt{s}=19$ GeV seems to disagree with the ISR data, presenting a too high value for $B=12.47\pm0.10$ GeV^{-2} (possibly because the measurements are taken at rather large momentum transfers; for our purposes these should be smaller than the hadronic scale of ≈1 GeV). This point at $\sqrt{s}=19$ GeV was taken as the sole input in the previous calculation [1].

In Fig. 1 we plot the two observables σ^T and B against each other. At the ISR energies we use

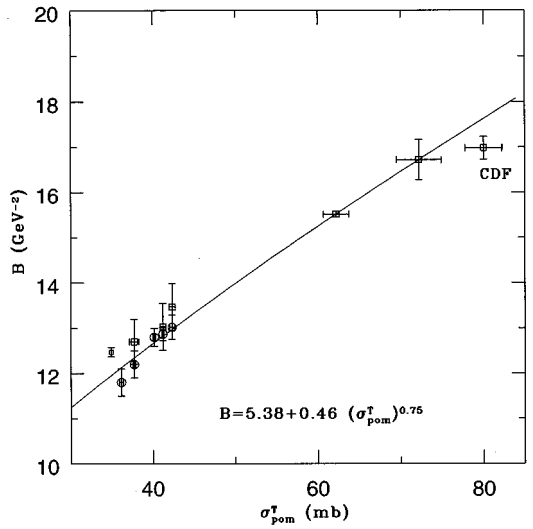

FIG. 1. Relation between the two experimental quantities of the pp and $\overline{pp}$ systems. The values of σ^T at energies up to 62.3 GeV shown in this figure are the $\sigma^T_{\rm Pom}$ values as given by the parametrization of Donnachie and Landshoff, namely $\sigma^T_{\rm Pom}=(21.70\ {\rm mb})s^{0.0808}$. We also included the point [10] at 19 GeV and the Fermilab CDF values [9] at 1800 GeV. The values of B for the pp system are shown with circles, while the values for $\overline{pp}$ are represented by squares. The solid line represents Eq. (1), with values for Δ, B_0, and C given in the figure.

$\sigma^T_{\rm pom}=(21.70{\rm mb})s^{0.0808}$ as representative of the nonperturbative contributions, instead of the full experimental values. At the highest energies (541–1800 GeV) it is believed that the process is essentially nonperturbative. The relation between the two observables is parametrized in the form

$$B=B_0+C(\sigma^T)^{\Delta}, \tag{1}$$

with $B_0=5.38$ GeV^{-2}, $C=0.458$ GeV^{-2}, $\Delta=0.75$, and with σ^T given in mb. This form is suggested by the results of the calculations with the model of the stochastic vacuum [1], where an interpretation for the meaning of the parameters is given in terms of QCD and hadronic quantities. This is explained in detail in Sec. IV.

In the next section we recall the principles of the evaluation of the observables of high-energy scattering in the model of the stochastic vacuum [1]. In the sections that follow we present our new calculations and results.

II. NONPERTURBATIVE QCD AND THE MODEL OF THE STOCHASTIC VACUUM IN SOFT HIGH-ENERGY SCATTERING

The nonperturbative vacuum expectation values (such as gluon condensates) that were first introduced in calculations of hadron spectroscopy [11] were shown by Nachtmann [12] to have fundamental role in soft high-energy scattering. The application of the model of the stochastic vacuum to this problem follows his general analysis, adopting however a different fundamental ingredient. Instead of reducing the hadron-hadron amplitude to quark-quark scattering amplitudes, the basic entities used are scattering amplitudes for Wilson loops in Minkowski space-time. The loops are formed by the trajectories of the quark and the antiquark of the hadronic system, and this approach has the important advantage that the amplitudes are gauge invariant.

The model of the stochastic vacuum [5] is based on the assumption that the low frequency contributions in the functional integral can be taken into account by a simple stochastic process with a converging cluster expansion [13]. The integration is specified by a simple correlator, which is determined by two scales: the strength of the correlator (the value of the gluon condensate) and the correlation length. This simple model leads to confinement in a non-Abelian

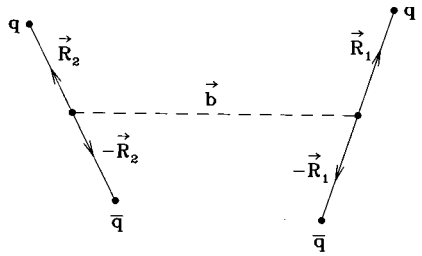

FIG. 2. View in the transverse plane of the two loops that represent the paths of quark and antiquark in meson-meson scattering. The vectors $\vec{R}_1$ and $\vec{R}_2$ represent components of the meson transverse wave functions. The vector $\vec{b}$ is the impact parameter vector connecting the geometric center of the two hadrons.

gauge theory, with a linear potential between static quarks which agrees with phenomenological determinations [14].

In order to guarantee gauge invariance, the model deals with the correlator of the field strengths $F_{\mu\nu}$, rather than with the expectation values of gauge potentials $A_\mu(x)$. In order to give a well-defined meaning to the correlator, which is a bilocal object, the color content of all fields must be parallel transported to a single reference point w. Then the parallel-transported field strength tensors

$$\mathbf{F}_{\mu\nu}(x;w) := \phi^{-1}(x,w)\mathbf{F}_{\mu\nu}(x)\phi(x,w), \tag{2}$$

where $\phi(x,w)$ is a non-Abelian Schwinger string from point w to point x, must be constructed. This quantity follows the gauge transformation at the fixed reference point w,

$$\mathbf{F}_{\mu\nu}(x,w) \to \mathbf{U}(w)\mathbf{F}_{\mu\nu}(x;w)\mathbf{U}^{-1}(w), \tag{3}$$

so that the vacuum expectation value $\langle \mathbf{F}_{\mu\nu}(x,w)\mathbf{F}_{\delta\sigma}(y,w)\rangle_A$ with respect to the low frequencies is a gauge invariant quantity.

With the approximation that the correlator is independent of the reference point w, depending only on the difference $z=x-y$, its most general form [5] is given by

$$\langle g^2 F^C_{\mu\nu}(x,w)F^D_{\rho\sigma}(y,w)\rangle_A = \frac{\delta^{CD}}{8}\frac{1}{12}\langle g^2FF\rangle\Bigg\{ \kappa(\delta_{\mu\rho}\delta_{\nu\sigma}-\delta_{\mu\sigma}\delta_{\nu\rho})D(z^2/a^2) + (1-\kappa)\frac{1}{2}\left[\frac{\partial}{\partial z_\mu}(z_\rho\delta_{\nu\sigma}-z_\sigma\delta_{\nu\rho})+\frac{\partial}{\partial z_\nu}(z_\sigma\delta_{\mu\rho}-z_\rho\delta_{\mu\sigma})\right]D_1(z^2/a^2)\Bigg\}. \tag{4}$$

Here a is a characteristic correlation length, $\langle g^2FF\rangle$ is the gluon condensate

$$\langle g^2FF\rangle = \langle g^2F^C_{\mu\nu}(0)F^C_{\mu\nu}(0)\rangle_A, \tag{5}$$

$C,D=1,\ldots,8$ are color indices, and the numerical factors in Eq. (4) are chosen in such a way that

$$D(0)=D_1(0)=1. \tag{6}$$

Lattice studies [15] show that the ratio $\kappa/(1-\kappa)$ is rather large (about 3), so that $D(z^2/a^2)$ gives the dominant contribution. This dominance was the reason for the previous [1] neglect of the contributions from the part $(1-\kappa)D_1(z^2/a^2)$, which are taken into consideration in the present work.

The correlator in Eq. (4) is the starting point for the evaluation of observables in soft high-energy scattering. In the analysis made by Nachtmann [12], the quark-quark scattering amplitude for the interaction of the quarks with the gluon field is evaluated using the eikonal approximation. If the energy of the quark is very high and the background field has only a limited frequency range, the quark moves on an approximately straight lightlike line and the eikonal approximation can be applied. In the limit of high energies there is helicity conservation and spin degrees of freedom can be ignored. This quark-quark scattering amplitude is explicitly gauge dependent. However, we can make use of the fact that in meson-meson scattering for each quark there is an antiquark moving on a nearly parallel line. The meson must be a color-singlet state under local gauge transformations, and to construct such a colorless state we have to parallel transport the color content from the quark to the antiquark. Since this parallel-transport of the colors is made by a Schwinger string, we obtain for the meson a rectangular Wilson loop whose lightlike sides are formed by the quark and antiquark paths, and whose front ends are the Schwinger strings. The direction of the path of an antiquark is effectively the opposite of that of a quark, so that the loop has a well-defined internal direction.

The resulting loop-loop amplitude is then specified, not only by the impact parameter, but also by the transverse extension vectors $\vec{R}_1$ and $\vec{R}_2$. In the transverse plane the two interacting loops are seen as shown in Fig. 2.

The functional integration over A is evaluated using the model of the stochastic vacuum. Since the correlator is given in terms of the parallel-transported field tensor $\mathbf{F}_{\mu\nu}(x,w)$, the line integrals $\int \mathbf{A}_\mu dz^\mu$ are transformed into surface integrals over the field tensor with the help of the non-Abelian Stokes theorem. The integrations are then extended over open surfaces S_1 and S_2 having the loops L_1 and L_2 as contours.

The exponential being expanded, the expectation value can be calculated assuming factorization in a Gaussian process. In the expansion of the trace of the exponential at least two terms are necessary, because $\mathrm{tr}\tau_A=0$, and the lowest order contribution to the loop-loop scattering amplitude is then given by

$$J(\vec{b},\vec{R}_1,\vec{R}_2) = -(-ig)^4\left(\frac{1}{2!}\right)^2 \mathrm{tr}[\tau_{C_1}\tau_{C_2}]\mathrm{tr}[\tau_{D_1}\tau_{D_2}]\int_{S_1}\prod_{i=1}^{2} d\Sigma^{\mu_i\nu_i}(x_i)\int_{S_2}\prod_{j=1}^{2} d\Sigma^{\rho_j\sigma_j}(y_j)\frac{1}{9} \times\langle F^{C_1}_{\mu_1\nu_1}(x_1,w)F^{C_2}_{\mu_2\nu_2}(x_2,w)F^{D_1}_{\rho_1\sigma_1}(y_1,w)F^{D_2}_{\rho_2\sigma_2}(y_2,w)\rangle_A + \text{higher correlators}. \tag{7}$$

The integration surfaces and details of the calculation have beeen described before [1]. The higher order terms are shown to be small as compared to the leading term, and can be neglected. In this approximation the surface ordering becomes irrelevant. The expectation values of the product of four fields is evaluated using the factorization hypothesis

$$\langle F^{C_1}F^{C_2}F^{D_1}F^{D_2}\rangle=\langle F^{C_1}F^{C_2}\rangle\langle F^{D_1}F^{D_2}\rangle+\langle F^{C_1}F^{D_1}\rangle \times\langle F^{C_2}F^{D_2}\rangle+\langle F^{C_1}F^{D_2}\rangle\langle F^{C_2}F^{D_1}\rangle. \tag{8}$$

It is convenient to introduce the eikonal function χ:

$$\chi(\vec{b},\vec{R}_1,\vec{R}_2)=(-ig)^2\int_{S_1}d\Sigma^{\rho\mu}(x)\int_{S_2}d\Sigma^{\sigma\nu}(y) \times\langle F^C_{\rho\mu}(x,w)F^C_{\sigma\nu}(y,w)\rangle_A. \tag{9}$$

Then the loop-loop amplitude $J(\vec{b},\vec{R}_1,\vec{R}_2)$ is given to the lowest order in the correlator by

$$J(\vec{b},\vec{R}_1,\vec{R}_2)=-\frac{1}{576}[\chi(\vec{b},\vec{R}_1,\vec{R}_2)]^2. \tag{10}$$

In order to extract as a factor the value of the gluon condensate, it is useful to introduce a reduced eikonal function and a reduced loop-loop scattering amplitude through

$$\widetilde{\chi}(\vec{b},\vec{R}_1,\vec{R}_2)\equiv\frac{12}{\langle g^2FF\rangle}\chi(\vec{b},\vec{R}_1,\vec{R}_2) \tag{11}$$

and

$$\widetilde{J}_{LL'}(\vec{b},\vec{R}_1,\vec{R}_2)\equiv\frac{1}{[\langle g^2FF\rangle]^2}J_{LL'}(\vec{b},\vec{R}_1,\vec{R}_2) =-\frac{[\widetilde{\chi}(\vec{b},\vec{R}_1,\vec{R}_2)]^2}{144\cdot 576}. \tag{12}$$

We have introduced the indices L,L' to indicate the two loops.

To be applied to high-energy scattering, the model of the stochastic vacuum must be translated from Euclidean spacetime, to the Minkowski continuum. The correlation functions $D(z^2/a^2)$ and $D_1(z^2/a^2)$ must fall off for negative z^2 values (corresponding to Euclidean distances), and must have well-defined Fourier transforms in the Minkowski metric, since these enter in the scattering amplitudes.

The loop-loop eikonal function is determined by the geometry of the two loops and by the form of the correlation functions. In Eq. (4) there appear two independent arbitrary scalar functions, $D(z^2/a^2)$ and $D_1(z^2/a^2)$, which are supposed to fall off at large distances with characteristic lengths a, called correlation lengths. Lattice calculations [15] show however that the forms of D and D_1 in the Euclidean region at large distances are similar (exponential decreases with same rates), with the contribution from the term with D in the correlator being about three times larger than that from D_1. We then adopt the same shapes $D\equiv D_1$, and $\kappa=3/4$.

A convenient general form [1] for the correlation function is

$$D^{(n)}(-|\vec{\xi}|^2)=\frac{1}{2^{n-3}\Gamma(n-3)}(\rho_n|\vec{\xi}|)^{n-3} \times\left[(n-1)K_{n-3}(\rho_n|\vec{\xi}|) -\frac{1}{2}(\rho_n|\vec{\xi}|)K_{n-2}(\rho_n|\vec{\xi}|)\right], \tag{13}$$

where $K_\nu(x)$ is the modified Bessel function, $n\geqslant 4$, and

$$\rho_n=\frac{3\sqrt{\pi}}{4}\frac{\Gamma(n-5/2)}{\Gamma(n-3)}. \tag{14}$$

The dependence of the final results on the particular choice for n is not very marked, the reason being that all correlation functions are normalized to 1 at the origin, and decrease exponentially at large distances. It is enough that the chosen function falls monotonicaly and smoothly in the range of physical influence (up to about 1 F, say), and there cannot be much difference in the results obtained using different reasonable analytical forms. The simpler choice is $n=4$, which in the Euclidean region leads to a good representation of the lattice calculations [15]. We then have for the correlation function

$$D^{(4)}(-|\vec{\xi}|^2)=(\rho_4|\vec{\xi}|)[K_1(\rho_4|\vec{\xi}|)-\tfrac{1}{4}(\rho_4|\vec{\xi}|)K_0(\rho_4|\vec{\xi}|)], \tag{15}$$

with

$$\rho_4=\frac{3\pi}{8}. \tag{16}$$

In the evaluation of the (Euclidean) Wilson loop in the model of the stochastic vacuum the D part of the correlator leads [5] to the area law for a Wilson loop, and to a relation involving the condensate $\kappa\langle g^2FF\rangle$, the correlation length a and the string tension ρ

$$\rho=\frac{\kappa\pi}{144}\langle g^2FF\rangle a^2\int_0^\infty D(-u^2)du^2. \tag{17}$$

For the family of correlators written above the integration can be performed analytically and for the case $n=4$ the result gives

$$\kappa\langle g^2FF\rangle=\frac{81\pi}{8a^2}\rho. \tag{18}$$

We thus say that D represents que confining correlator, while D_1 is the nonconfining (and Abelian) part.

After the limits are taken, which make the long sides of the rectangular Wilson loops tend to $\pm\infty$ in the direction of the colliding beams, the remaining variables in the integrands are coordinates of points in the transverse plane. The distances z between such points enter in the final expressions for the eikonal functions χ as arguments of the two-dimensional inverse Fourier transform, which is given by

$$\mathcal{F}_2^{(4)}(-|\vec{\xi}|^2)=\frac{32}{9\pi}(\rho_4|\vec{\xi}|)^2\left[2K_0(\rho_4|\vec{\xi}|)-\left(\frac{4}{\rho_4|\vec{\xi}|}-\rho_4\left|\vec{\xi}\right|\right)K_1(\rho_4|\vec{\xi}|)\right]$$
$$=-\frac{32}{9\pi}\Delta_2[(\rho_4|\vec{\xi}|)^3K_3(\rho_4|\vec{\xi}|)], \qquad (19)$$

where Δ_2 is the two-dimensional Laplacian operator, and $\vec{\xi}$ is any two-dimensional vector of the transverse plane and K_3 is a modified Bessel function. This Laplacian form is important in the calculation, as it allows lowering the order of the integrations, through Gauss theorem.

III. PROFILE FUNCTION FOR HADRON-HADRON SCATTERING

We now introduce the notation $\vec{R}(I,J)$, where the first index ($I=1,2$) specifies the loop, and the second specifies the particular quark or antiquark ($J=1$ or 2) in that loop.

Figure 3 shows a projection on the transverse scattering plane. The vectors $\vec{Q}(K,L)$ in the transverse plane connect the reference point C (with coordinates w) to the positions of the quarks and antiquarks of the loops 1 and 2. The quantity $\psi(K,L)$ is the angle between $\vec{Q}(1,K)$ and $\vec{Q}(2,L)$.

In the evaluation of the eikonal functions $\chi[\vec{b},\vec{R}(1,1),\vec{R}(2,1)]$ coming from the confining case a typical resulting contribution is

$$\int_0^1 d\alpha\int_0^1 d\beta\cos\Psi(1,1)\mathcal{F}_2^{(4)}[-|\alpha\vec{Q}(1,1)-\beta\vec{Q}(2,1)|^2], \qquad (20)$$

where $\mathcal{F}_2^{(4)}$ is the above-mentioned two-dimensional Fourier transform of the correlator with $n=4$. Taking advantage of the Laplacian form, we can apply Gauss' theorem in two dimensions and eliminate one further integration. The term from the nonconfining correlator has a total derivative under the integration sign, and in this part one more integration can be immediately made.

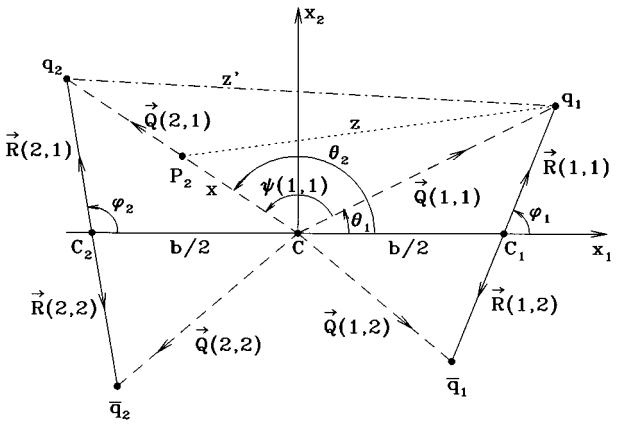

FIG. 3. Geometrical variables of the transverse plane, which enter in the calculation of the eikonal function for meson-meson scattering. The points C_1 and C_2 are the meson centers. In the integration P_2 runs along the vector $\vec{Q}(2,1)$, changing the length z, which is the argument of the characteristic correlator function. In analogous terms, points P_1, $\overline{P_1}$, and $\overline{P_2}$ run along $\vec{Q}(1,1)$, $\vec{Q}(1,2)$, and $\vec{Q}(2,2)$. This explains the four terms that appear inside the brackets multiplying κ in the expression for the loop-loop amplitude. The length z' of the dot-dashed line is the argument of the Bessel function arising from the nonconfining correlator D_1; there are four such terms, appearing inside the brackets multiplying $(1-\kappa)$.

We then write for the eikonal function of the loop-loop amplitude

$$\tilde{\chi}(\vec{b},\vec{R}(1,1),\vec{R}(2,1))=\kappa[-\cos\psi(1,1)I[Q(1,1),Q(2,1),\psi(1,1)]-\cos\psi(2,2)I[Q(1,2),Q(2,2),\psi(2,2)]$$
$$+\cos\psi(1,2)I[Q(1,1),Q(2,2),\psi(1,2)]+\cos\psi(2,1)I[Q(1,2),Q(2,1),\psi(2,1)]]$$
$$+(1-\kappa)[-W[Q(1,1),Q(2,1),\psi(1,1)]-W[Q(1,2),Q(2,2),\psi(2,2)]+W[Q(1,1),Q(2,2),\psi(1,2)]$$
$$+W[Q(1,2),Q(2,1),\psi(2,1)]]. \qquad (21)$$

The quantities I which represent the non-Abelian contributions are given by integrations along the dashed lines of the figure:

$$I[Q(1,K),Q(2,L),\psi(K,L)]=\frac{32}{9\pi}\left(\frac{3\pi}{8}\right)^2\left\{Q(1,K)\int_0^{Q(2,L)}[Q(1,K)^2+x^2-2xQ(1,K)\cos\psi(K,L)]K_2\right.$$
$$\times\left[\frac{3\pi}{8}\sqrt{Q(1,K)^2+x^2-2xQ(1,K)\cos\psi(K,L)}\right]dx$$
$$+Q(2,L)\int_0^{Q(1,K)}[Q(2,L)^2+x^2-2xQ(2,L)\cos\psi(K,L)]K_2$$
$$\left.\times\left[\frac{3\pi}{8}\sqrt{Q(2,L)^2+x^2-2xQ(2,L)\cos\psi(K,L)}\right]dx\right\}, \qquad (22)$$

with $Q(K,L)=|\vec{Q}(K,L)|$. The quantities W, which come from the nonconfining part of the correlator, are given by

$$W[Q(1,K),Q(2,L),\psi(K,L)]=\frac{32}{9\pi}2\frac{3\pi}{8}[Q(1,K)^2+Q(2,L)^2-2Q(1,K)Q(1,L)\cos\psi(K,L)]^{3/2}$$
$$\times K_3\left[\frac{3\pi}{8}\sqrt{Q(1,K)^2+Q(2,L)^2-2Q(1,K)Q(2,L)\cos\psi(K,L)}\right]. \quad (23)$$

From the eikonal function $\tilde{\chi}$ we contruct the loop-loop amplitude $\tilde{J}_{L_1L_2}(\vec{b},\vec{R}_1,\vec{R}_2)$, where $\vec{R}_1$ and $\vec{R}_2$ are shorthand notation for $\vec{R}(1,1)$ and $\vec{R}(2,1)$, respectively.

The hadron-hadron amplitude is constructed from the loop-loop amplitude using a simple quark model for the hadrons. Since our amplitude is independent of the momentum of the quarks (as long as the energy is high enough to ensure lightlike paths), the dependence of the wave functions on the longitudinal momenta of the quarks can be neglected, and we thus only consider the transverse dependence, which is given by the Fourier transform of the transverse wave function. We thus obtain the hadron-hadron scattering amplitude by smearing over the values of $\vec{R}_1$ and $\vec{R}_2$ in Eq. (10) with transverse wave functions $\psi(\vec{R})$.

Taking into account the results of the previous analysis of different hadronic systems [1], in the present calculation we only consider for the proton a diquark structure, where the proton is described as a meson, in which the diquark replaces the antiquark. Thus these expressions apply equally well to meson-meson, meson-baryon, and baryon-baryon scattering.

For the hadron transverse wave function we make the ansatz of the simple Gaussian form

$$\psi_H(R)=\sqrt{2/\pi}\frac{1}{S_H}\exp(-R^2/S_H^2), \quad (24)$$

where S_H is a parameter for the hadron size.

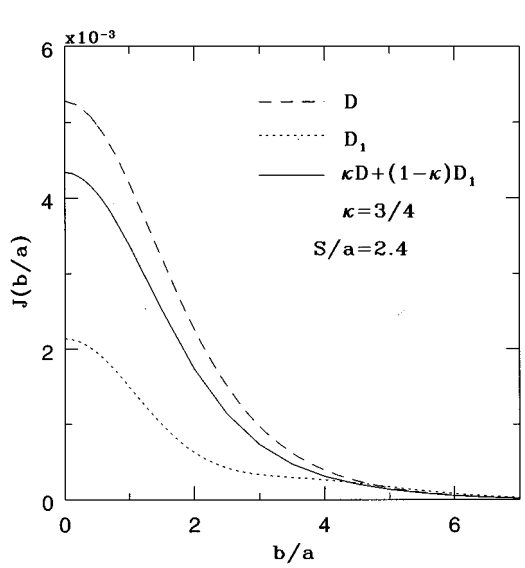

FIG. 4. Dimensionless profile functions $J(b/a)$ for $S/a=2.4$ obtained in the cases of pure confining ($\kappa=1$), pure nonconfining ($\kappa=0$), and mixed ($\kappa=3/4$) correlators.

We then write the reduced profile function of the eikonal amplitude

$$\hat{J}_{H_1H_2}(\vec{b},S_1,S_2)=\int d^2\vec{R}_1\int d^2\vec{R}_2\tilde{J}_{L_1L_2}(\vec{b},\vec{R}_1,\vec{R}_2)$$
$$\times|\psi_1(\vec{R}_1)|^2|\psi_2(\vec{R}_2)|^2, \quad (25)$$

which is a dimensionless quantity.

For short, from now on we write $J(b)$ or $J(b/a)$ to represent $\hat{J}(\vec{b},S_1,S_2)$.

In the present work the contributions of both the confining and nonconfining correlators to the eikonal function and to the observables in high-energy scattering are taken into account. Aiming at the pp and $\overline{pp}$ systems, we only consider the case $S_1=S_2=S$. Figure 4 shows a comparison between the results for the profile functions $J(b/a)$ corresponding to $S/a=2.4$ in the cases of pure confining ($\kappa=1$), pure nonconfining ($\kappa=0$), and mixed ($\kappa=3/4$) correlators, in order to exhibit their differences. The smaller contributions at the physically more important values of b/a obtained in the nonconfining case justified its neglect in previous work.

We have studied analytically the profile functions for very large values of b/a and found that the asymptotic behavior is of the form

$$J(b/a)=\exp\left(-\frac{3\pi}{8}\frac{b}{a}\right)\left[\frac{A_1}{b/a}+\frac{A_2}{b/a^2}+\ldots\right], \quad (26)$$

where $A_1,A_2,\ldots$ are functions of S/a.

For small and intermediate values of b/a, $J(b/a)$ can be written, in good approximation [1], as a Gaussian exponential multiplied by a rational fraction on $(b/a)^2$. For the whole range, a parametrization which can be made very faithful is of the form

$$J(b/a)=J(0)\left[\frac{A_0}{1+C_0(b/a)^2}\exp[-P(b/a)^2]\right.$$
$$\left.+\sum_{j=1}^{N}\frac{A_j}{1+C_j(b/a)^j\exp[(3\pi/8)(b/a)]}\right], \quad (27)$$

where $\Sigma_{j=0}^{N}A_j=1$. The parameters P, A_j, C_j depend on S/a, and can be determined by fitting the exact (numerically obtained) values of $J(b/a)$. For practical purposes $N\leqslant 3$.

The dimensionless hadron-hadron scattering amplitude in the eikonal approach is given by

$$T_{H_1H_2}=is[\langle g^2FF\rangle a^4]^2a^2\int d^2\vec{b}\exp(i\vec{q}\cdot\vec{b})\hat{J}_{H_1H_2}(\vec{b},S_1,S_2), \quad (28)$$

where the impact parameter vector $\vec{b}$ and the hadron sizes S_1 and S_2 are in units of the correlation length a, and $\vec{q}$ is the momentum transfer projected on the transverse plane, in units of $1/a$, so that the momentum transfer squared is $t=-|\vec{q}|^2/a^2$. For convenience, in the expression above we have explicitly factorized the dimensionless combination $\langle g^2FF\rangle a^4$. The normalization for $T_{H_1H_2}$ is such that the total cross-section is obtained through the optical theorem by

$$\sigma^T=\frac{1}{s}\mathrm{Im}T_{H_1H_2}, \tag{29}$$

and the differential cross section is given by

$$\frac{d\sigma^{el}}{dt}=\frac{1}{16\pi s^2}|T_{H_1H_2}|^2. \tag{30}$$

To write convenient expressions for the observables, we define the dimensionless moments of the profile function (as before, with b in units of the correlation length a)

$$I_k=\int d^2\vec{b}b^kJ(b), \quad k=0,1,2,\ldots, \tag{31}$$

which depend only on S/a, and the Fourier-Bessel transform

$$I(t)=\int d^2\vec{b}J_0(ba\sqrt{|t|})J(b), \tag{32}$$

where $J_0(ba\sqrt{|t|})$ is the zeroth-order Bessel function. Then

$$T_{H_1H_2}=is[\langle g^2FF\rangle a^4]^2a^2I(t).$$

Since $J(b)$ is real, the total cross section σ^T, the slope parameter B (slope at $t=0$) and the differential elastic cross section are given by

$$\sigma^T=I_0[\langle g^2FF\rangle a^4]^2a^2, \tag{33}$$

$$B=\frac{d}{dt}\left(\ln\frac{d\sigma^{el}}{dt}\right)\bigg|_{t=0}=\frac{1}{2}\frac{I_2}{I_0}a^2=Ka^2, \tag{34}$$

and

$$\frac{d\sigma^{el}}{dt}=\frac{1}{16\pi}I(t)^2[\langle g^2FF\rangle a^4]^4a^4. \tag{35}$$

We have here defined

$$K=\frac{1}{2}\frac{I_2}{I_0}.$$

We observe that in the lowest order of the correlator expansion the slope parameter B does not depend on the value of the gluon condensate $\langle g^2FF\rangle$ and, once the proton radius S is known, may give a direct determination of the correlation length.

The QCD strength and length scale have been factorized in the expressions for the observables, and the correlation length appears as the natural unit of length for the geometric aspects of the interaction. These aspects are contained in the quantities $I_0(S/a)$ and $I_2(S/a)$, which depend on the hadronic structures and on the shapes and relative weights (parameter κ) of the two correlation functions. It has been shown [1] that for the case $\kappa=1$ the two moments have simple form as functions of S/a. To consider arbitrary values for κ, we remark that the profile function and its moments are quadratic functions of κ, as they result from integrations of the squares of a (symbollic) combination $\kappa D+(1-\kappa)D_1$. The profile function $J(b/a)$ for an arbitrary value of the weight κ can be obtained once the profile functions have been determined for three different values of κ. It is shown in the next section that the moments $I_0(S/a)$ and $I_2(S/a)$ for arbitrary κ (with $0\leqslant\kappa\leqslant1$) can be represented by similarly simple expressions.

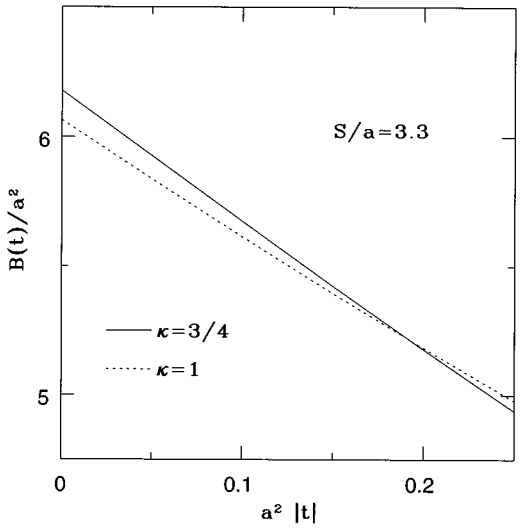

FIG. 5. t dependence of the slope parameter $B(t)$ for the cases $\kappa=3/4$, 1.

It is important that the high-energy observables σ^T and B require only the two low moments I_0 and I_2 of the profile functions. The curvature of the forward peak depends on higher moments and on the long distance behavior of $J(b/a)$.

The t dependence of the logarithmic slope of the differential cross section is given by

$$B(t)=\frac{d}{dt}\left(\ln\frac{d\sigma^{el}}{dt}\right)=\frac{2}{I(t)}\frac{dI(t)}{dt}$$

$$=\frac{1}{I(t)}\frac{a}{\sqrt{|t|}}\int_0^\infty 2\pi J(b)b^2J_1(ba\sqrt{|t|})db. \tag{36}$$

The form of $B(t)$, which is exemplified in Fig. 5 for $\kappa=1$ and 3/4, depends of the behavior of the profile function for large values of b/a. The present form of the calculations with the model of the stochastic vacuum, with its simplifying schemes, and reasonable but arbitrary ansatz for the correlation functions, should not be expected to give detailed description of quantities depending on the long range behavior of the profile function. The experimental quantities for large momentum transfers are sensitive to this behavior.

TABLE II. Values of the parameters for Eqs. (37) and (38), for some selected values of κ.

κ	$\alpha\times10^2$	β	η	γ	δ	δ/β
1/2	0.6880	2.474	2.283	0.3906	2.016	0.815
3/4	0.6532	2.791	2.030	0.3293	2.126	0.762
33/40	0.6409	2.895	1.973	0.3190	2.161	0.746
1.0	0.6717	3.029	1.859	0.3118	2.183	0.721

IV. EXPERIMENTAL OBSERVABLES AND QCD PARAMETERS

The curves for $I_0=\sigma^T/[\langle g^2FF\rangle^2 a^{10}]$and $K=B/a^2$ can be parametrized as functions of S/a with simple powers, with good accuracy for $0\leqslant\kappa\leqslant1$. The convenient expressions are

$$I_0=\alpha\left(\frac{S}{a}\right)^{\beta} \tag{37}$$

and

$$K=\eta+\gamma\left(\frac{S}{a}\right)^{\delta}. \tag{38}$$

The parameters $\alpha,\beta,\eta,\gamma,\delta$ and the ratio δ/β (which is of particular importance for the comparison with the data) are shown as functions of κ in Figs. 6 and 7. Their numerical values for some selected values of κ are given in Table II.

The parametrizations of the total cross section and of the slope parameter B are very convenient for comparison of the results of the model of the stochastic vacuum with experiment. In order to have a wide range of data to extract reliable information on QCD parameters, we concentrate on elastic pp and $p\overline{p}$ scattering. The data extending from the ISR range (20–60 GeV) to the Fermilab energy (1800 GeV) are presented in Table I and in Fig. 1.

The nonperturbative calculation made with the model of the stochastic vacuum corresponds to the phenomenological Pomeron exchange of Regge phenomenology [2,3]. Donnachie and Landshoff [3] found that the parametrization

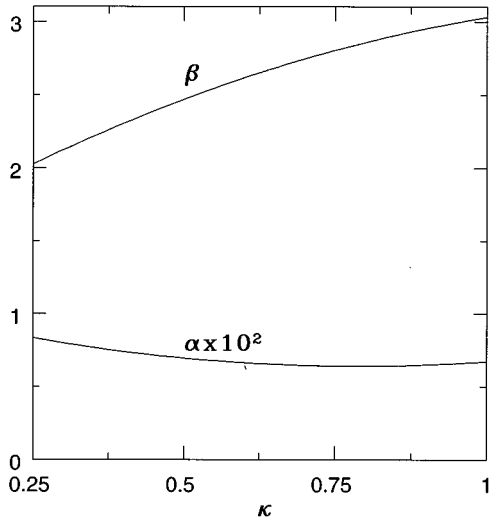

FIG. 6. Values of $\alpha\times10^2$ and β as functions of κ.

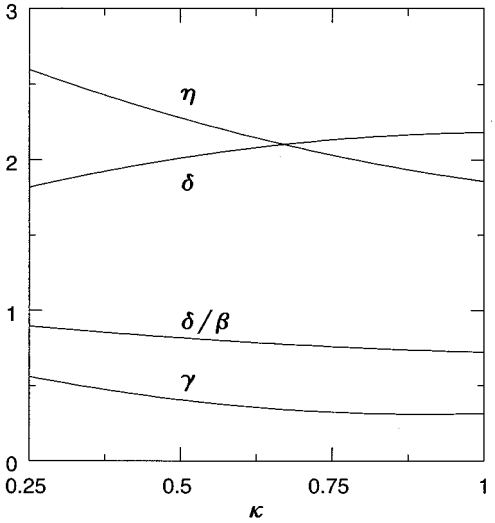

FIG. 7. Values of η, γ, and δ and δ/β as functions of κ.

$\sigma^T_{\rm Pom}(pp,p\overline{p})=(21.70\ {\rm mb})s^{0.0808}$ (with s in GeV^2) works well over a wide range of data above $\sqrt{s}=5$ GeV, so that we may use this expression to represent the pomeron contribution at the energies where the non-Pomeron part is important (the ISR energies). At 541 and 1800 GeV we assume that Pomeron exchange dominates the scattering process, and ignore possible differences between pp and $p\overline{p}$ systems. We then take the data at these two highest energies as input, and predict the values for the lower (ISR) energies.

The values of the slope parameter related to the Pomeron exchange mechanism are not known, and must be predicted by a model. Our model makes specific predictions for the relation between $\sigma^T_{\rm Pom}$ and $\mathrm{B}_{\rm Pom}$, and we need good data to test accurately these predictions. The differences $B(p\overline{p})-B(pp)$ are 0.50, 0.16, and 0.45 GeV^{-2} at 30.5, 52.7, and 62.3 GeV, respectively, with error bars typically $\pm0.55\ \mathrm{GeV}^{-2}$ (see Table I); these differences do not show a decrease with the increasing energy, as expected from Pomeron dominance, but the error bars are too large, larger than the quantities themselves. The situation is simpler with the total cross sections, where at the same three energies the differences $\sigma^T(p\overline{p})-\sigma^T(pp)$ are 2.02, 0.94, and 0.57 mb, respectively, decreasing continously to zero, and with error bars not larger than the values of the differences. Thus, in the range of the ISR experiments, we see the cross sections converging to the same Pomeron-exchange values, but not the slopes.

In Fig. 1, besides the ISR and higher-energy data, we show the point [10] corresponding to $\sqrt{s}=19$ GeV with $\sigma^T_{\rm Pom}=34.92$ mb and $B=12.47\pm0.10\ \mathrm{GeV}^{-2}$. This point has been used [1] as an input in a previous application of the model of the stochastic vacuum to high-energy scattering, and we now see that it is not consistent (due to a too large value for B) with the ISR data, as shown in Fig. 1. This consideration has influence in the numerical values that are obtained for the QCD parameters. In Fig. 1 we show also the Fermilab CDF values at 1800 GeV, which must be considered as *alternative* to the values obtained in the E-710 experiment, since they refer to the same energy; in the analysis presented below we opt for the E-710 values, which fit more naturally in our calculation.

Once the forms of the correlation functions are fixed, the parameters in the model that are fundamentally related to QCD are the weigth κ, the gluon condensate $\langle g^2FF\rangle$, and the correlation length a. The hadronic extension parameter S_H accounts for the energy dependence of the observables. In this section we show how these quantities can be evaluated using exclusively high-energy scattering data.

To obtain from Eqs. (33), (34), (37), and (38) a relation between the observables σ^T and B at a given energy, we eliminate the radius, and write

$$(B-\eta a^2)=\frac{a^2}{(\langle g^2FF\rangle a^4)^{2\delta/\beta}}\frac{\gamma}{\alpha^{\delta/\beta}}\left(\frac{\sigma^T}{a^2}\right)^{\delta/\beta}. \qquad (39)$$

The form of Eq. (39) is the same as given by Eq. (1), with an obvious correspondence of parameters.

To determine the parameters, we first remark that the exponent $\Delta=\delta/\beta$ does not depend on QCD quantities and is almost constant (equal to about 3/4) in the region of values of κ that are obtained in lattice calculations ($\kappa\approx 3/4$). This tells us that we cannot easily extract a unique value of κ from high-energy scattering data only, but tells us also that the power Δ in Eq. (1) must surely be very close to

$$\delta/\beta=\Delta=3/4. \qquad (40)$$

This is a fortunate result for our analysis, because then in practice we are left with only two free quantities in both energy independent relations (39) and (1). They can be determined using as input the two clean experimental points for σ^T and B at 541 and 1800 GeV given in Table I. We then obtain

$$B_0=\eta a^2=5.38\ \text{GeV}^{-2}=0.210\ \text{fm}^2,\quad C=0.458\ \text{GeV}^{-2}. \qquad (41)$$

Figure 1 shows the observables of soft high-energy scattering, with the modification that for the total cross sections at the ISR energies we show the nonperturbative Pomeron-exchange contribution $\sigma^T_{\text{Pom}}(pp,\overline{pp})=(21.70\ \text{mb})s^{0.0808}$ instead of the full experimental value. The values of B for the pp system are shown with circles, while the values for $\overline{pp}$ are represented by squares. The solid line is Eq. (1), with values for Δ, B_0, and C given above. We see that using the 541 and 1800 GeV data as input, the model gives a very good prediction for the ISR data. It is interesting to observe that the values of B for the pp system are closer to our prediction for the nonperturbative slope (the solid line) compared to the $\overline{pp}$ values, which are rather high.

Equation (39) gives the correspondence between the phenomenological quantities Δ, B_0, C and the parameters of the model and of QCD. Since the model parameters are functions of κ only, we can also obtain the QCD parameters as functions of κ. They are plotted in Figs. 8 and 9. The correlation length is remarkably constant, while the gluon condensate decreases as κ increases.

Of course these results are subject to uncertainties. We have adopted an ansatz for the correlation function, which is arbitrary (although numerically it could not be very different). There is some uncertainty also in the determination of the parameters $\alpha,\beta\ldots$ representing the final results of the numerical calculation. On the other hand, the model gives a rather unique prediction for $\Delta=\delta/\beta=3/4$ which is well sustained by the data as shown in Fig. 1.

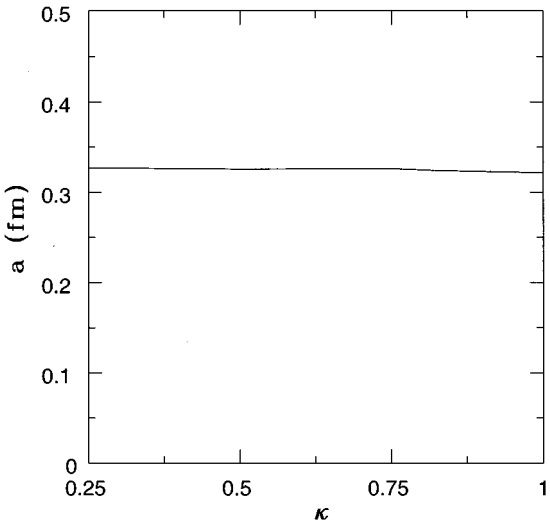

FIG. 8. The correlation length as a function of κ. The values are determined using as input the data at 541 and 1800 GeV.

To be specific, we borrow from lattice calculation the value $\kappa=3/4$, and then use as parameter values the numbers shown in Table II. Taking into account the experimental error bars in the input data at 541 and 1800 GeV, we obtain

$$\kappa=3/4,\quad a=0.32\pm 0.01\ \text{fm},$$

$$\langle g^2FF\rangle a^4=18.7\pm 0.4,\quad \langle g^2FF\rangle=2.7\pm 0.1\ \text{GeV}^4. \qquad (42)$$

With the value $\kappa=33/40$ obtained in more recent lattice results [16] the central values change slightly to

$$\kappa=33/40,\quad a=0.33\ \text{fm},$$

$$\langle g^2FF\rangle a^4=19.2,\quad \langle g^2FF\rangle=2.6\ \text{GeV}^4. \qquad (43)$$

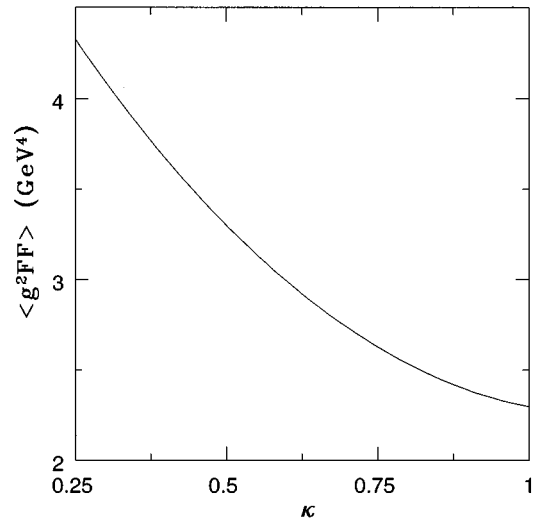

FIG. 9. The gluon condensate $\langle g^2FF\rangle$ as a function of κ, determined using as input the data at 541 and 1800 GeV.

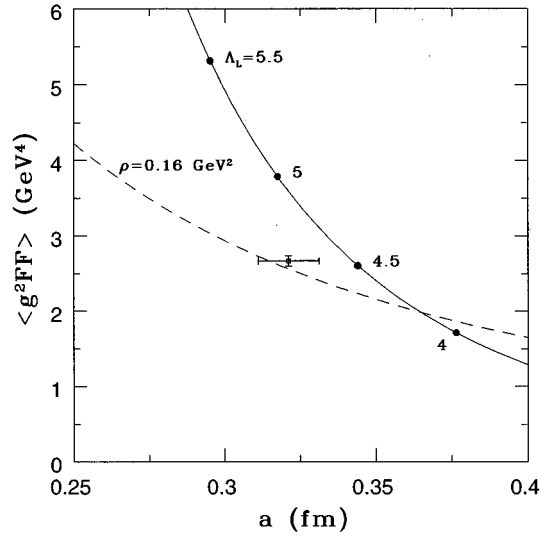

FIG. 10. Constraints on the values of $\langle g^2FF\rangle$ and of the correlation length a. The solid line is the fit of our correlator to the lattice calculation [15] as given in Eq. (44). The dashed line plots Eq. (18), with $\rho=0.16$ GeV^2. The cross centered at $a=0.32$ fm, $\langle g^2FF\rangle=2.7$ GeV^4 shows the result of our calculation given in Eq. (42).

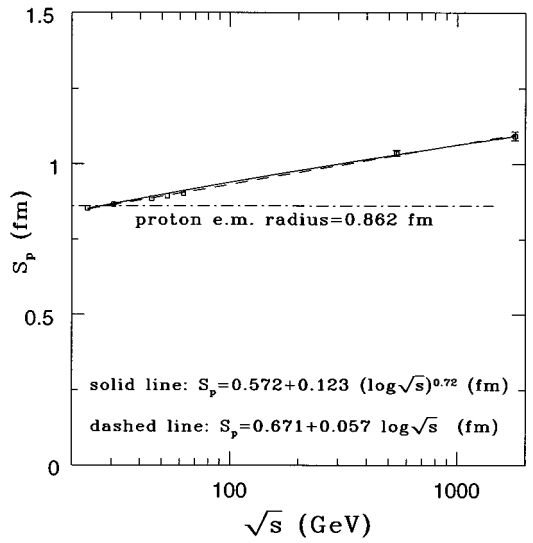

FIG. 11. Energy dependence of the proton radius. The marked points are obtained from the total cross section data (at the ISR energies the total cross-sections are represented by the Pomeron exchange contributions). The two representations for the radius dependence are indistinguishable with the present data, but give quite different predictions for the cross-section values at the LHC energies.

The results of the pure SU(3) lattice gauge calculation by Di Giacomo and Panagopoulos [15] for the correlator $\langle F^C_{\mu\nu}(x,0)F^D_{\rho\sigma}(0,0)\rangle_A$ have been fitted [1] with the same correlation function (15) used in the present work. The correlation between the values of $\langle g^2FF\rangle$ and a that was then obtained can be well represented by the empirical expressions

$$\Lambda_L=\frac{1.1122}{a^{1.310}},\quad \langle g^2FF\rangle=\frac{0.018\,13}{a^{4.656}},$$

$$\langle g^2FF\rangle a^4=0.0172\sqrt{\Lambda_L}, \tag{44}$$

with the lattice parameter Λ_L in MeV, a in fm, and $\langle g^2FF\rangle$ in GeV^4. This correlation is displayed in Fig. 10, where some chosen values of Λ_L are marked. Λ_L usually takes values in the range 5 ± 1.5 MeV. The point representing our results of Eq. (42) is marked in the same figure. The dashed line represents the relation between the gluon condensate, the correlation length and the string tension obtained in the application of the model of the stochastic vacuum [5] to hadron spectroscopy; for our form of correlator, this relation is given by Eq. (18). The curve drawn corresponds to a string tension $\rho=0.16$ GeV^2 .

As can be seen from the figure, the constraints from these three independent sources of information are simultaneously satisfied, providing a consistent picture of soft high-energy pp and $\overline{p}p$ scattering. The (pure gauge) gluon condensate is well compatible with the expected value. The lattice parameter Λ_L and the string tension ρ are also in their acceptable ranges. As we describe below, the resulting proton size parameter S_p takes values quite close to the electromagnetic radius [17].

In our model the increase of the observables with the energy is due to a slow energy dependence of the hadronic radii. An explicit relation is obtained if we bring into Eqs. (33) and (37) a parametrization for the energy dependence of the total cross sections, such as the Donnachie-Landshoff [3] form. In this case we obtain for the proton radius

$$S_p(s)=a\frac{1}{\alpha^{1/\beta}}\frac{1}{(\langle g^2FF\rangle a^4)^{2/\beta}}\left(\frac{21.7\ \text{mb}}{a^2}\right)^{1/\beta}s^{0.0808/\beta}. \tag{45}$$

The energy dependence, given by a power $0.0808/\beta$ of s is very slow, and the values obtained for S_p are in the region of the proton electromagnetic radius [17], which is $R_p=0.862\pm0.012$ fm. However, use of the Donnachie-Landshoff parametrization for the total cross sections is not appropriate at very high energies. Using Eqs. (33) and (37) and directly the data at 541 and 1800 GeV, we obtain the values for the proton radius that are shown in Fig. 11, where a log scale is used for $\sqrt{s}$. It is remarkable that we have an almost linear dependence, which can be represented by

$$S_p(s)=0.671+0.057\ln\sqrt{s}(\text{fm}), \tag{46}$$

with $\sqrt{s}$ in GeV. With this form for the radius, which is shown in dashed line in Fig. 11, the cross sections evaluated at very high energies rise with a term $\ln^\beta\sqrt{s}$, and are smaller than predicted by the power dependence of Donnachie and Landshoff. However, since $\beta\approx2.8$, they still violate the bound $\ln^2\sqrt{s}$. This may be corrected using a power $2/\beta$ instead of 1 in the parametrization for $S_p(s)$, and we then obtain

$$S_p(s)=0.572+0.123[\ln\sqrt{s}]^{0.72}(\text{fm}). \tag{47}$$

This form is shown in solid line in Fig. 11. Clearly it gives a good representation for the existing data. At 14 TeV, which is the expected energy in the future experiments, at the

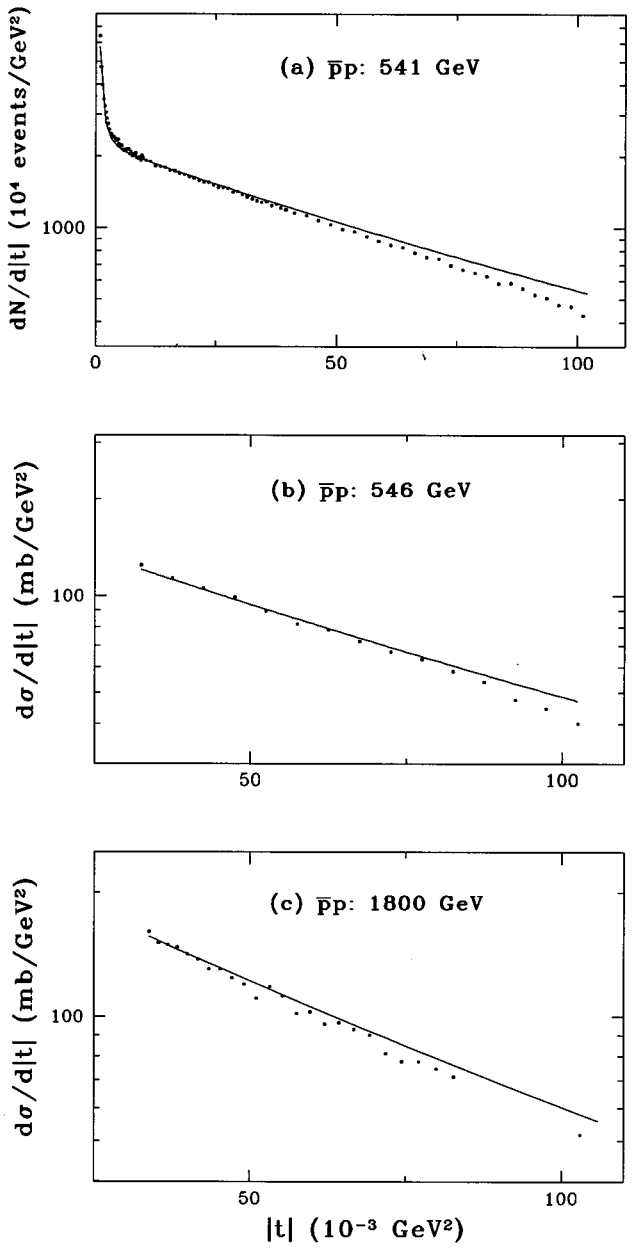

FIG. 12. Elastic differential cross sections at high energies [6]. The solid lines represent the calculations with the model of the stochastic vacuum described in the present work, without free parameters. The systematic deviations occurring for $|t|$ larger about 30×10^{-3} GeV^2 arise from the long range behavior of the profile function $J(b/a)$.

CERN Large Hadron Collider (LHC) we obtain $S_p(14\ \text{TeV})=1.19$ fm $=1.38$, $R_p=3.7a$, and the model predictions for the observables are $\sigma^T=92$ mb and $B=19.6$ GeV^{-2}. The dashed line representing Eq. (46) leads at the same LHC energy to $\sigma^T=97$ mb and $B=20.1$ GeV^{-2}, while the Donnachie-Landshoff formula leads to the still higher value $\sigma^T=101.5$ mb.

The nonperturbative QCD contributions to soft high-energy scattering are expected to be dominant in the forward direction, thus determining the total cross section (through the optical theorem) and the forward slope parameter. The model, as it is presented in this paper, leads to a negative curvature for the slope $B(t)$, which decreases as $|t|$ increases, as shown in Fig. 5. The data however show an almost zero curvature of the peak, so that above some value of $|t|$ the model leads to too high values of the differential cross section. This is illustrated in Fig. 12, where the experimental data [6] at 541, 546, and 1800 GeV are shown, together with the results of the model, without any free parameter (the gluon condensate, the correlation length and the hadronic radius have been uniquely fixed by the inputs of σ^T and B at 541 and 1800 GeV).

Rather small changes in the form of the profile function $J(b)$ that enters in the expression for the scattering amplitude, particularly changing the shape of $J(b)$ at large b [notice that the curvature is determined by a high moment I_4 in Eq. (31)] are able to modify this behavior. This can be made phenomenologically, introducing a form factor [18]. However, in the present work we wish to keep the fundamental characteristics of the model, which is that of a pure QCD based calculation, with a unique set of quantities governing all systems at all energies.

V. CONCLUSIONS

We have extended the previous calculation of soft high-energy scattering, now including the two tensor forms in the correlator, and thus taking into account the two independent correlation functions. We study the influence of the weight parameter κ that measures the ratio between the two contributions, giving the general results that allow the determination of the observable quantities and QCD parameters in terms of this weight. We show that there are little changes in the final results, when κ varies in the ranges suggested by lattice determinations.

We describe the most important data on total cross section and slope parameter for the pp and $\overline{pp}$ systems, extended

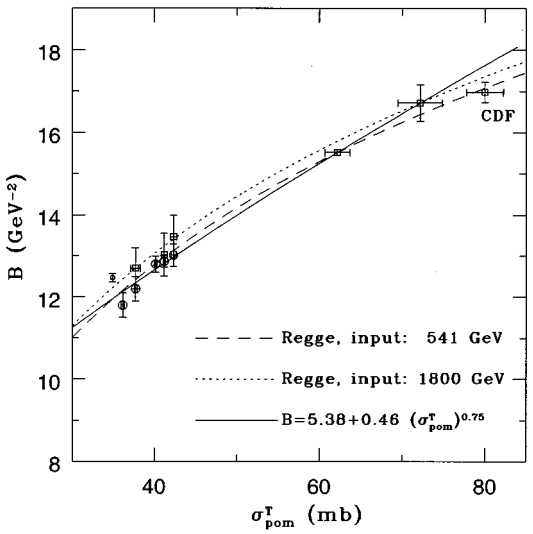

FIG. 13. Relation between observables of high-energy scattering obtained in our calculations compared to the relation obtained from a Regge amplitude according to Eq. (48). The dashed line uses as input for the Regge formula the $\sqrt{s}=541$ GeV data and passes close to the CDF point at 1800 GeV. The dotted line uses as input the values of the E-701 experiment at $\sqrt{s}=1800$ GeV.

from $\sqrt{s} \approx 20$ to 1800 GeV, giving a unified and consistent description of these data in terms of fundamental quantities. The nonperturbative QCD parameters determining the observables are the gluon condensate and the correlation length of the vacuum field fluctuations. The third quantity entering the calculations is the transverse hadron size, which has a magnitude close to the electromagnetic radius, and whose variation accounts for the energy dependence of the observables.

The model allows a very convenient factorization between the QCD and hadronic sectors. Elimination of the hadron size parameter between the expressions for the two observables at a given energy yields a parameter-free and energy independent relation between the total cross section and the slope of the elastic cross section which agrees very well with experiment. Starting from two experimental energies as input, this expression gives a prediction of the remaining data, and leads to a determination of the correlation length and the gluon condensate from high-energy data alone. The results obtained are in good agreement with the correlations between the two QCD parameters obtained in the lattice calculations and in the application of the stochastic vacuum model to hadronic spectroscopy.

In the expansion of the exponential with functional integrations, the present calculation is restricted to the lowest order nonvanishing contribution, which is quadratic in the gluonic correlator, and we may conclude from our results that this is justified for the evaluations of total cross section and slope parameter. The resulting amplitude is purely imaginary, and the ρ parameter (the ratio of the real to the imaginary parts of the elastic scattering amplitude) can only be described if we go one further order in the contributions to the correlator. Also the factorization in Eq. (8), implied by the assumption of a Gaussian process, is important in the present formulation of the model, and possibly has consequences for the phenomenological analysis.

It is interesting to compare our results with Regge phenomenology. In Fig. 13 we plot the relation between the observables given by

$$\sigma_{\mathrm{Regge}}^{T} = \sigma_{0}^{T} e^{0.1616(B-B_0)}, \tag{48}$$

obtained from a Regge amplitude using the slope of the Pomeron trajectory $\alpha'(0)_{\mathrm{Pom}} = 0.25\ \mathrm{GeV}^{-2}$. This relation requires an input pair σ_0^T, B_0 at a chosen energy. The dashed line uses as input the $\sqrt{s} = 541$ GeV data $\sigma_0^T = 62.20$ mb, and $B_0 = 15.52\ \mathrm{GeV}^{-2}$. It is interesting to observe the tendency of this line to pass close to the CDF experimental point, instead of the E-710 point. The dotted line uses as input the values of the E-701 experiment at $\sqrt{s} = 1800$ GeV and shows a deviation at 541 GeV. This is rather intriguing, as it implies that Eq. (48) favors the CDF experimental results at 1800 GeV.

ACKNOWLEDGMENTS

Part of this work was done while one of the authors (E.F.) was visiting CERN, and he wishes to thank the Theory Division for the hospitality. The authors are indebted to H. G. Dosch for extensive and helpful discussions. Both authors thank CNPq (Brazil) and FAPERJ (Rio de Janeiro, Brazil) for financial support.

[1] H. G. Dosch, E. Ferreira, and A. Krämer, Phys. Lett. B **289**, 153 (1992); **318** 197 (1993); Phys. Rev. D **50**, 1992 (1994).

[2] P.D.B. Collins, *An Introduction to Regge Theory and High Energy Physics* (Cambridge University Press, Cambridge, England, 1977).

[3] A. Donnachie and P. V. Landshoff, Phys. Lett. B **296**, 227 (1992).

[4] B. Povh and J. Hüfner, Phys. Rev. Lett. **58**, 1612 (1987); Phys. Lett. B **215**, 772 (1988); **245**, 653 (1990); Phys. Rev. D **46**, 990 (1992); C. Bourrely, J. Soffer, and T. T. Wu, Nucl. Phys. **B247**, 15 (1984); Phys. Rev. Lett. **54**, 757 (1985); Phys. Lett. B **196**, 237 (1987); J. Dias de Deus and P. Kroll, Nuovo Cimento A **37**, 67 (1977); Acta Phys. Pol. B **9**, 157 (1978); J. Phys. G **9**, L81 (1983); P. Kroll, Z. Phys. C **15**, 67 (1982); T. T. Chou and C. N. Yang, Phys. Rev. **170**, 1591 (1968); Phys. Rev. D **19**, 3268 (1979); Phys. Lett. **128B**, 457 (1983); *ibid.* **244**, 113 (1990); E. Levin and M. G. Ryskin, Sov. J. Nucl. Phys. **34**, 619 (1981).

[5] H. G. Dosch, Phys. Lett. B **190**, 177 (1987); H. G. Dosch and Yu. A. Simonov, *ibid.* **205**, 339 (1988).

[6] Main references to the data. (a) N. Amos *et al.*, Nucl. Phys. **B262**, 689 (1985); (b) R. Castaldi and G. Sanguinetti, Annu. Rev. Nucl. Part. Sci. **35**, 351 (1985); (c) C. Augier *et al.*, Phys. Lett. B **316**, 448 (1993); (d) M. Bozzo *et al.*, *ibid.* **147B**, 392 (1984); M. Bozzo *et al.*, *ibid.* **147B**, 385 (1984); (e) N. Amos *et al.*, *ibid.* **247**, 127 (1990); Phys. Rev. Lett. **68**, 2433 (1992); Fermilab Report No. FN-562 [E-710] 1991 (unpublished).

[7] Data Compilations: Particle Data Group, L. Montanet *et al.*, Phys. Rev. D **50**, 1173 (1994); Review Articles: L. L. Jenkovszky, Fortschr. Phys. **34**, 791 (1986); M. M. Block and R. N. Cahn, Rev. Mod. Phys. **57**, 563 (1985).

[8] G. Alner, Z. Phys. C **32**, 153 (1986).

[9] F. Abe *et al.*, Phys. Rev. D **50**, 5550 (1994); **50**, 5518 (1994).

[10] J. B. Burq *et al.*, Nucl. Phys. **B217**, 285 (1983).

[11] M. A. Shifman, A. I. Vainshtein and V. I. Zakharov, Nucl. Phys. **B147**, 385 (1979); **B147**, 448 (1979); **B147**, 519 (1979).

[12] O. Nachtmann, Ann. Phys. (N.Y.) **209**, 436 (1991).

[13] N. G. van Kampen, Physica **74**, 215 (1974); **74**, 239 (1974); Phys. Rev. C **24**, 172 (1976); G. C. Hegerfeldt and H. Schulze, J. Stat. Phys. **51**, 691 (1988).

[14] M. Schiestl and H. G. Dosch, Phys. Lett. B **209**, 85 (1988); Y. A. Simonov, Nucl. Phys. **B234**, 67 (1989).

[15] A. Di Giacomo and H. Panagopoulos, Phys. Lett. B **285**, 133 (1992).

[16] A. Di Giacomo, E. Maggiolaro, and H. Panagopoulos, Institution Report No. hep-lat/9603017, 1996 (unpublished).

[17] Proton radius: G. G. Simon *et al.*, Z. Naturforsch. A **35**, 1 (1980).

[18] U. Grandel and W. Weise, Phys. Lett. B **356**, 567 (1995).